TEMPERATURE-RESPONSIVE POLY(VINYL ALCOHOL)-BORAX SALOGELS FOR SHAPE STABILIZATION OF AN INORGANIC PHASE CHANGE MATERIAL

A Thesis

by

XIUZHU ZHU

Submitted to the Graduate and Professional School of
Texas A&M University
in partial fulfillment of the requirements for the degree of

MASTER OF SCIENCE

Chair of Committee,	Svetlana Sukhishvili
Committee Members,	Patrick Shamberger
	Emily Pentzer
	Jodie Lutkenhaus
Head of Department,	Ibrahim Karaman

December 2021

Major Subject: Materials Science and Engineering

ABSTRACT

A temperature-responsive gel has been introduced to achieve shape stabilization of phase change materials (PCMs). Inorganic salt hydrates are promising PCMs, but their low viscosity at temperatures above their melting point leads to leakage and corrosion in thermal storage modules. Temperature-responsive salogels can trap inorganic salt hydrates to achieve shape stabilization when the temperature is lower than the gel-sol transition temperature (T_{gel}) to overcome the leakage problem. Increasing the temperature above T_{gel} transforms the system to the liquid state enabling easy removal of the PCM material from the thermal storage units. This work focuses on the salogels system consisting of poly(vinyl alcohol) (PVA) dissolved in calcium nitrate tetrahydrate (CNH). Through variations in molecular weight, degree of hydrolysis, and concentration of PVA, precise control of T_{gel} of the salogel was achieved. Importantly, at the matched PVA concentrations, gelation occurred in CNH but not in water. This difference is rationalized by the unique features of CNH as a solvent, such as an extremely high salt content and scarcity of water. Interactions of PVA and solvent were investigated using attenuated total reflection Fourier Transform Infrared spectroscopy (ATR-FTIR), and a suggested mechanism of gelation of PVA in CNH is discussed. To further enhance the salogel strength and improve control over the gelation temperature, borax as a crosslinker that forms dynamic covalent bonds with PVA was introduced. PVA/borax/CNH salogels could achieve T_{gel} as high as 70^{o}C using 3 wt% PVA and as low as ~0.3 wt% concentration of borax. The crosslinking mechanism of borax and PVA in CNH involves formation of

dynamic covalent borate ester bonds, which lead to salogel strengthening. Compared to traditional PVA-borax hydrogels in water, PVA-borax salogels in CNH showed the unique feature of highly repeatable temperature reversibility. In addition, the reported salogels not only provide shape stabilization of CNH but also exhibit robust self-healing properties.

ACKNOWLEDGEMENTS

I would like to thank my committee chair, Dr. Sukhishvili, and my committee member, Dr. Shamberger, Dr. Pentzer, and Dr. Lutkenhaus, for their guidance and support throughout this research.

I would like to give special thanks to my friends and colleagues and the department faculty and staff for making my time at Texas A&M University a great experience.

Finally, I am thankful to my mother and father for their encouragement and love.

CONTRIBUTORS AND FUNDING SOURCES

Contributors

This work was supervised by chair of my thesis committee Dr. Sukhishvili, with significant contributions of Dr. Shamberger (Department of Materials Science & Engineering).

The DSC data for heat of fusion was tested by Sourav Chakravarty.

ATR-FTIR and rheology data collection and analysis were done in collaboration with Kartik Kumar Rajagopalan.

Funding Sources

This work was supported by U.S. Department of Energy's Office of Energy Efficiency and Renewable Energy (EERE) under the Buildings and Technologies Award Number DE-EE0009155.

NOMENCLATURE

PVA	Poly(vinyl alcohol)
$PVA_{H,98}$	High molecular weight, hydrolysis percent 98%
$PVA_{M,98}$	Medium molecular weight, hydrolysis percent 98%
$PVA_{H,87}$	High molecular weight, hydrolysis percent 87%
PCMs	Phase change materials
CNH	Calcium nitrate tetrahydrate
LNH	Lithium nitrate tetrahydrate
T_{gel}	Gel-sol transition temperature
ATR-FTIR spectroscopy	Attenuated total reflection Fourier Transform Infrared
DSC	Differential scanning calorimetry

TABLE OF CONTENTS

Page

LIST OF FIGURES

Page

LIST OF TABLES

Page

1. INTRODUCTION

1.1. PCMs

In the past two decades, much attention has been paid to thermal energy storage as a powerful enabler for renewable energy technologies, such as thermal solar energy and waste heat recovery.[1] PCMs have been widely considered in energy storage because of their high energy density and isothermal operation.[2] Application of PCMs in the building thermal management include incorporation of PCMs in the building walls or other components of the buildings, or use of PCMs in the heat and cold storage units.[3]

PCMs can be categorized as organic, inorganic, and eutectics. Inorganic PCMs show many advantages, such as higher heat storage capacities, lower costs, and non-flammability as compared to organic PCMs.[4] Salt hydrates, composed of inorganic salt and water forming crystalline solid, $AB \cdot nH_2O$, are the most important group of inorganic PCMs. Upon melting of crystal hydrates, water is released from the solid and hydrates dissolved ions. However, n moles of water released from the crystals upon melting is not sufficient to saturate the hydration shells of all ions in solution. This water-starved state of ions in molten inorganic PCM is a distinct feature that makes these liquids a unique media for dissolution of organic compounds and polymers.

This work employed calcium nitrate tetrahydrate (CNH) – an inorganic salt hydrate with heat of fusion of 153 kJ/kg and a near-ambient melting temperature of 42^{o}C.[3] CNH is inexpensive and readily available commercially, but suffers a problem of low viscosity typical of inorganic salt hydrates that leads to leakage problems during their

applications as PCMs. [5] Therefore, temperature-responsive salogels formed by polymers in inorganic salt hydrates have been used to achieve shape stabilization during the PCM melting/freezing cycles.[6, 7]

1.2. PVA

In this work, PVA has been dissolved in CNH to form a polymer network of a salogel. PVA is a synthetic and non-toxic polymer, which has been employed in biomedical industry, mostly due to its excellent water solubility.[8, 9] Despite its synthetic character, this polymer also was recognized as biodegradable.[10] PVA cannot be prepared by direct polymerization of vinyl alcohol, and is instead obtained by hydrolysis of poly(vinyl acetate) by reacting this polymer with methanol under alkaline conditions. Depending on the degree of hydrolysis, different PVA types can be produced with distinct physical properties. PVA is typically soluble in water, but its solubility is dependent on the polymer molecular weight, degree of hydrolysis, and crystallinity.[11] Polymer molecular weight and degree of hydrolysis also play significant roles in gelation of this polymer in water. For instance, various degrees of hydrolysis suggest hierarchical polymer-solvent and polymer-polymer interactions, which are critical in gelation.[12]

1.3. Salogels and gelation mechanism

Salogels present a temperature-responsive matrix that provides shape stabilization for inorganic PCMs.[6, 7] They can transform from gel to the liquid as temperature rises above the gel-sol transition temperature (T_{gel}). This transition facilitates the processes of filling in and removal of a PCM material from the thermal storage module after the lifecycle expiration. Temperature-responsive salogels belong to the class of physical gels.

Examples of physical gels formed in aqueous environment include PEG-based hydrogels, poly(N-isopropylacrylamide) (PNIPAm)-based hydrogels, among others.[13, 14] In these systems, gelation occurs when a 3D network of polymers is formed due to physical crosslinking via hydrogen bonding, van der Waals forces, hydrophobic or electrostatic interactions, or through entanglements of polymer chains. [15, 16] The salogels in this work are quite different from physical gels formed in aqueous solution (i.e. hydrogels) because they are formed in extremely salty CNH medium.

1.4. CNH as a unique solvent

In our group's previous work, salogels have been introduced to shape stabilize lithium nitrate tetrahydrate (LNH).[6, 7] It was found that LNH worked as a unique solvent resulting in gelation of PVA, which does not occur in water at any concentration of PVA.[17] CNH is another unique solvent with high ion content and scarcity of water. Each calcium nitrate tetrahydrate ($Ca(NO_3)_2 \cdot 4H_2O$) crystal hydrate contains 3 ions (one Ca^{2+}, two NO_3^-) and 4 water molecules. The number of waters released during melting of CNH crystal hydrate is not enough to hydrate all the ions, therefore ions are partially hydrated or in the contact ion-pairing state.[18-21] Therefore, when a polymer is added to the salt hydrate solvent, the interactions between the ions, polymer, and water govern the solvation and gelation of polymers in these solvents.[17]

1.5. Borate ester bond

In this work, the salogels formed by the addition of only PVA to CNH were weak, with T_{gel} lower than the melting point of CNH of 42°C. An increase in PVA concentration improved T_{gel} but resulted in diminishing of the heat of fusion of the system.

Consequently, an appropriate crosslinker was required to increase T_{gel} and strengthen the salogels. Typically, physical crosslinkers are widely used in other systems to enhance the gel network and maintain the temperature-responsive property.[22-24] Borax is often used as a crosslinker in 1,2 or 1,3 cisdiols-based hydrogel system, that forms dynamic borate ester bonds to build a stronger network structure and introduce stretchability and self-healability into the system.[25, 26] So PVA/borax hydrogels are widely applied in tissue engineering, biomedical areas, and 3D-printing.[27-29] The dynamic borate ester bond can easily dissociate under external stimuli, such as pH and temperature. [27, 30, 31] Therefore, we propose using borax to form dynamic covalent bonds with PVA to keep the temperature-responsive property in this work.

During the PVA-borax crosslinking reaction, borax dissociates into borate ions and boric acid first (eq (1) and eq (2)) in aqueous medium. This is followed by binding of borate ions with two diol units to form the didiol-borax complex in two steps (eq (3) and eq (4)).

$$Na_2B_4O_7 + 7H_2O \rightarrow 2B(OH)_3 + 2B(OH)_4^- + 2Na^+ \quad (1)$$

$$B(OH)_3 + 2H_2O \rightleftharpoons B(OH)_4^- + H_3O^+ \quad (2)$$

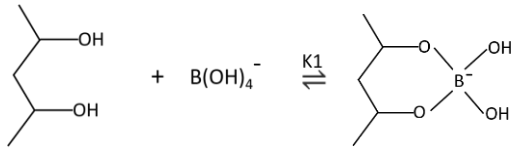

(3)

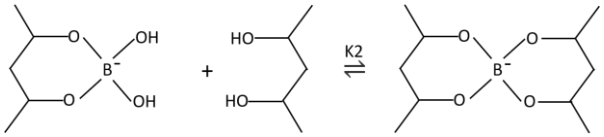

(4)

Based on eq 2, changing system pH can tune the number of borate ions, which affects the number of crosslinking points in PVA-borax gel. The pH-responsiveness has been confirmed in many PVA-borax hydrogel systems.[27, 32, 33] However, PVA-borax salogels in CNH show unique property of temperature-repeatability.

In this work, we explored the effect of PVA molecular weight and degree of hydrolysis on temperature responsive PVA/CNH salogels. We were interested in the interactions between water, ions, and PVA, and focused on understanding of the mechanism by which the divalent cation salt hydrate solvent controls formation and temperature-triggered destruction of the salogel network. We showed that the covalent dynamic borate ester bonds yielded strong yet reversible binding of crosslinkers and the polymer network. As a result, salogels could maintain their macroscopic shape stabilization and exhibited robust self-healing behavior but could be reversibly decomposed by increasing temperature at the same time. Most importantly, only a small amount of PVA and tiny amount of crosslinker was required to obtain shape stabilization during freezing/melting cycles, allowing to maintain most of heat of fusion of CNH as a phase change material.

2. EXPERIMENTAL

2.1. Materials

$PVA_{H,98}$ (Mw 88−97 kg /mol, hydrolysis percent 98%), $PVA_{M,98}$ (Mw 57−66 kg/mol, hydrolysis percent 98%), $PVA_{H,87}$ (Mw 88−97 kg/mol, hydrolysis percent 87%), sodium tetraborate decahydrate (ACS, 99.5-105.0%), boric acid (99+%), and glycerol (99+%) were purchased from Alfa Aesar and used as received. Calcium nitrate tetrahydrate (ACS, 99.0-103.0%) was purchased from Alfa Aesar and purified by passing through a PTFE (0.45µm, 40mm) syringe filter. Deuterium oxide (D_2O) with 99.9 atom % was purchased from Sigma-Aldrich and used as received. Ammonium hydroxide (28-30%) and hydrochloric acid (36.5-38%) were purchased from VWR International.

2.2. Preparation of salogels

Liquid CNH was obtained by heating solid CNH up to 50^{o}C in a sealed vial. PVA/CNH salogels were prepared by adding various PVA powders into liquid CNH to achieve different polymer concentrations. Then the mixtures were heated to 80^{o}C on a hot plate and subjected to gentle stirring for 24 hours in a sealed vial. After the PVA was completely dissolved, stirring was stopped, and the samples were put into the oven at 80^{o}C for 24 hours to remove bubbles and obtain a homogeneous mixture. The samples were then cooled down to room temperature to induce gelation. PVA/borax/CNH salogels were prepared by adding borax to PVA/CNH salogel at 70^{o}C, followed by heating the mixture to 90^{o}C while stirring to facilitate the dissolution of borax, and cooling down to room temperature to induce gelation. Because of the known supercooling effect that is

significant in the case of CNH,[3] no crystallization occurred in the system at room temperature.

2.3. Deuterated CNH for ATR-FTIR

Using D_2O instead of H_2O in the salt hydrate enables distinguishing the -OH stretching band of PVA and water band of the salt hydrate. Deuterated CNH (CND) was obtained by replacing the water with deuterium oxide in CNH. Firstly, the calcium nitrate tetrahydrate was heated in a vacuum oven at 135^{o}C to remove water and form anhydrous calcium nitrate. Then CND was obtained by mixing anhydrous calcium nitrate salt with the stoichiometric amount of deuterium oxide. Analysis by Attenuated total reflection Fourier transform infrared spectroscopy (ATR-FTIR) showed the disappearance of -OH peak (2100-2800 cm^{-1}) and the appearance of -OD peak (3000-3800 cm^{-1}), which confirmed the successful deuteration of CNH.

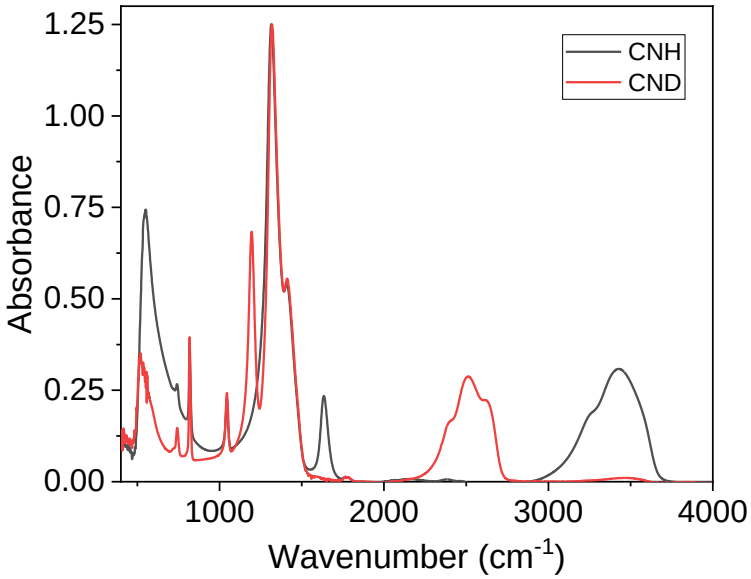

Figure 2.1. ATR-FTIR spectrum of CNH and CND

2.4. Characterization Techniques

2.4.1. Attenuated Total Reflection Fourier Transform Infrared Spectroscopy

Attenuated total reflection Fourier transform infrared spectroscopy (ATR-FTIR) measurements were performed using a Bruker Tensor II spectrometer equipped with a mercury cadmium telluride (MCT) detector and a single-reflection diamond ATR attachment. Spectra was collected in the range of 400-4000 cm^{-1} with 4 cm^{-1} resolution using 64 repetitious scans.

2.4.2. Rheological Measurements.

An Anton Paar stress-controlled rheometer (MCR 301) equipped with a Peltier stage that enabled controlling the temperature within ±0.5 °C was used to run the oscillation shear measurements with all salogel samples. All measurements were performed using parallel plate with a 40 mm diameter and the gap of 800 μm. The linear viscoelastic regime (γ_L) was determined by oscillation amplitude sweep tests which were conducted at 25 °C within a strain range of 0.1−100% using a frequency of 10 rad/s. The oscillation temperature ramp and oscillation frequency were tested in the linear viscoelastic regime. The oscillation time sweeps were alternatively conducted at linear and non-linear regime to illustrate the self-healing property. To minimize water evaporation and absorption, a solvent trap was used during the experiments.

2.4.3. Thermal Analysis

The melting temperatures and heat of fusion of PVA-based salogels were determined by differential scanning calorimetry (DSC) using a TA Instruments Q2000.

Measurements were conducted at a 10 °C/min temperature ramp from -20°C to 90°C under nitrogen gas purging at a flow rate of 50 mL/min.

3. RESULTS AND DISCUSSION

3.1. Gelation mechanism

At equal PVA concentrations (5 wt%), gelation occured in CNH but not in H_2O because of the different polymer-solvent and polymer-polymer interactions in the two solvents (Fig. 3.1). PVA dissolution requires heating to above 95^{o}C with vigorous stirring in water, whereas in CNH, heating up to 80^{o}C with gentle stirring was sufficient. The difference in solubility and chain morphology of PVA in H_2O and CNH are due to the characteristics of solvents. In water, PVA solvation is governed by water-polymer and polymer-polymer interactions. For CNH as a solvent, solvation water is scarce, solubility and gelation of polymers in CNH are primarily determined by the balance of ion-polymer and polymer-polymer with water-polymer interactions.

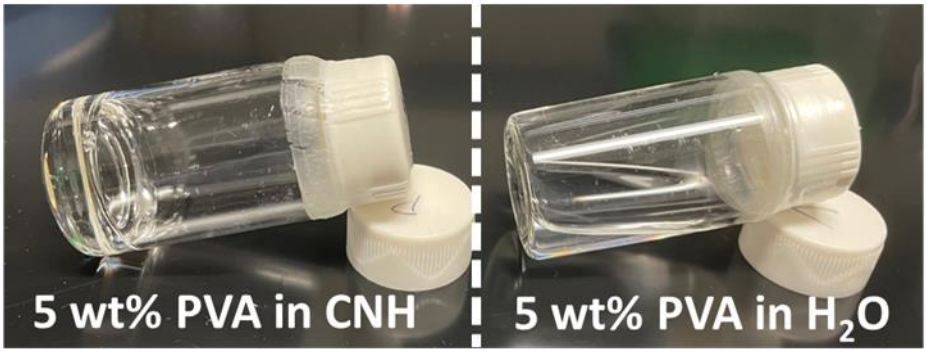

Figure 3.1. 5 wt% $PVA_{H,98}$ in CNH and H_2O

ATR-FTIR analysis of CND was investigated to understand the state of hydration of ions from the OD peak (2100-2800 cm^{-1}). Peak fitting of the OD peak of D_2O was done based on Sun's 5 sub-bands theory[34] which considers single donor double acceptor (DAA, strong), double donor double acceptor (DDAA, strong), double donor single acceptor

(DDA, weak), single donor single acceptor (DA, weak) hydrogen bonding modes, and free OD (Fig 3.2a) giving origin to the vibrational features of water. The fitting results were obtained by assuming the 5-sub peaks are Gaussian. For D_2O fitting, the peak centers and bandwidths were not fixed to get the parameters, but the results of the sub-peaks were carefully checked with previously published works.[35, 36] Then, the parameters from D_2O were used to fit the most similar sample to obtain a suitable initial fitting. Unfixed all the parameters in the following to finish the final fitting. Before curve fitting, a baseline correction was performed to the raw spectra. From the theoretical study of water clusters to bulk water, DDAA hydrogen bonding preferably occurs in larger water clusters like $(H_2O)_{16}$, $(H_2O)_{20}$. In contrast, DA hydrogen bonding preferably occurs in smaller water cluster, $(H_2O)_{6,}$ etc.[37, 38] Comparing the OD stretching vibrational region (Fig. 3.2b & c), the OD peak dramatically differs in D_2O and liquid CND, indicating the different state of water in these two solvents. Addition of D_2O to CND results in a decrease in DA and increase in DDAA hydrogen bonding modes (Fig. 3.2d). This means that smaller water cluster are gathering into larger water cluster, emphasizing that the first hydration shell of ions does not contain enough D_2O for completing ion hydration in CND. The analysis of the peak positions in the spectra of CND and aqueous salt solution shows that DA and DDA modes showed a significant red-shift upon an increase in D_2O content (Fig. 3.3), while DAA and DDAA do not show a significant change. Because when the water molecule in DA or DDA hydrogen bonding motif, the oxygen atom in water molecule only behaves as acceptor once, which makes them easy to interact with cations, especially when the cations are not fully hydrated. In general, from the analysis of D_2O vibrational

peaks, we know that water in CND is scarce for ion hydration. Most water molecules have strong bonding with ions, and ion shells have high electron density due to their incomplete hydration.

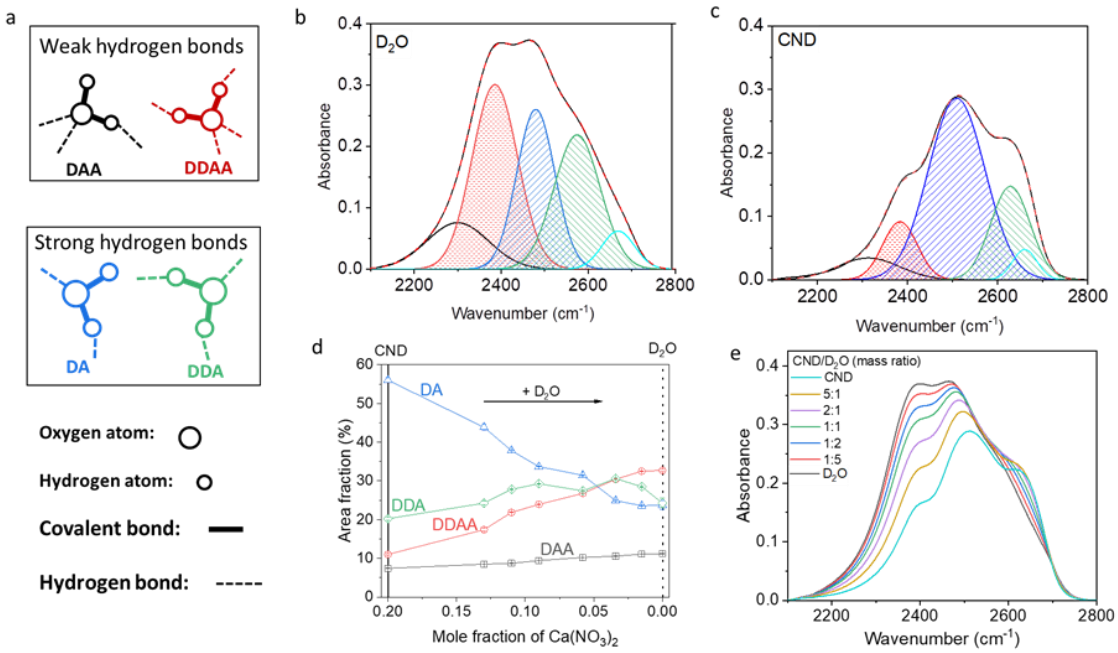

Figure 3.2. ATR-FTIR analysis of 2100-2800 cm^{-1} OD stretching vibrational band in D_2O and CND. (a) Schematic of DAA, DDAA, DA, and DDA hydrogen bonding motifs; (b) D_2O and (c) CND spectra fitting; (d) the observed spectroscopic changes in the OD vibrational region, and (e) their quantification through area fractions of the sub-peaks.

The next question that was addressed is how the addition of polymer, and specifically PVA affects the structure of the solvent. Because PVA could not be dissolved in CNH at concentrations exceeding 8%, glycerol was used as a model molecule due to its structural similarity to PVA to mimic the interactions of the hydroxyl groups of PVA in CNH. By using glycerol instead of PVA, large glycerol concentrations could be achieved which allowed to sensitively monitor spectral changes in the OD vibrational range of the solvent (2200-2800 cm^{-1}) and in the OH stretching vibrational range of glycerol (3000-

3800 cm^{-1}) at different glycerol dilution levels in glycerol-CND and glycerol-CND-D_2O systems (Figs. 3.4). The former case, the ratio of glycerol and CND was changed, revealing how glycerol concentration affects water state and the interaction between glycerol and CND. In the latter case, glycerol concentration was kept constant at amole fraction at 0.15, while the ratio of CND and D_2O was varied, revealing the effect of water content on spectal feature and hydration of glycerol.

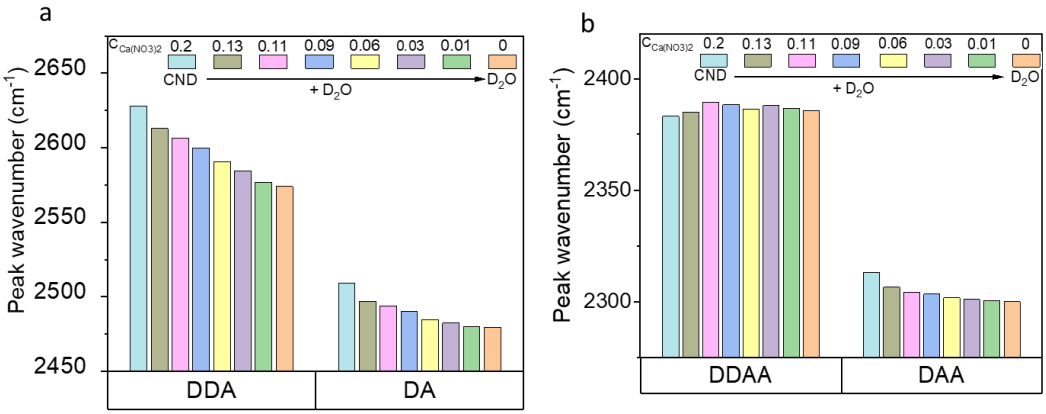

Figure 3.3. Sub-peaks wavenumber changes in CND-D_2O mixtures.

Investigation of the area fraction of sub-peaks of OD band in glycerol-CND mixtures (Fig. 3.4b) showed that upon an increase in concentration of glycerol in CND solutions, relative contributions of DA and DDAA hydrogen bonding motifs to the OD stretching region increased. In comparison, the free OD group, DAA, and DDA hydrogen bonding motifs disappear gradually. These results are indicating competition between glycerol and ions for water molecules. At the same time, increasing D_2O content in glycerol-CND-D_2O at a fixed glycerol concentration (Fig. 3.4c) showed a similar trend as adding D_2O to CND (Fig. 3.2d), i.e. a decrease in absorbances of DA hydrogen bonding and an increase in absorbances of DDAA hydrogen bonding motifs. As water content

increases, existing glycerol has negligible effect on the water state because water is no longer scarce for ions and glycerol hydration. Therefore, the use of CND as a solvent for glycerol leads to dehydrated glycerol state. Because of water scarcity, glycerol needs to compete with ions for hydration by water molecules. This has an important consequence for PVA gelation in CNH.

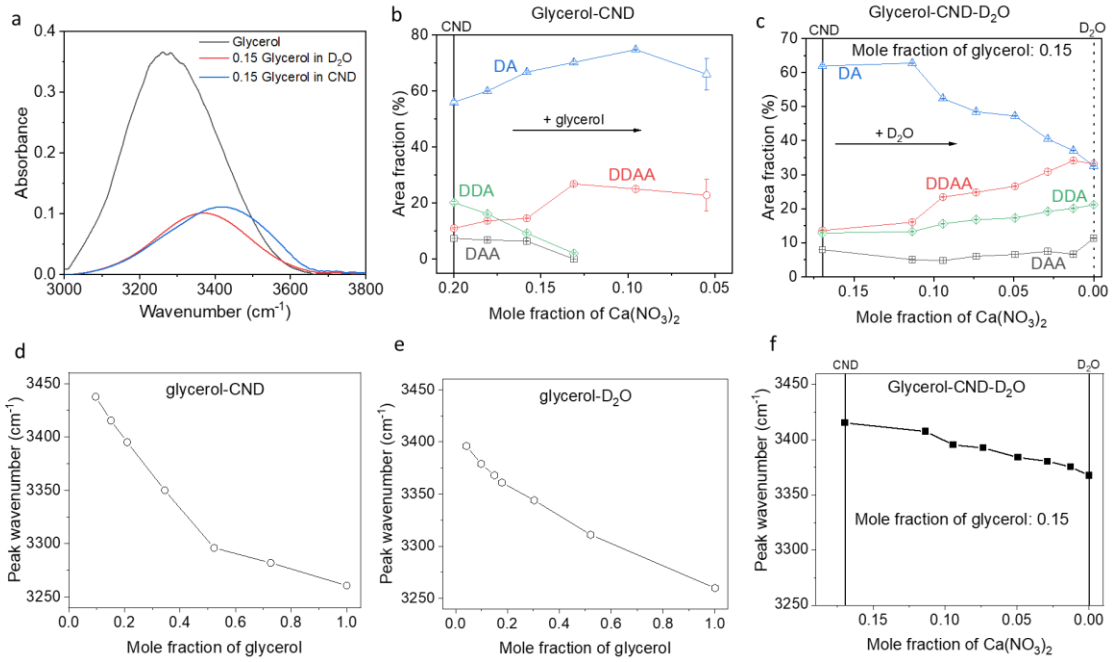

Figure 3.4. (a) ATR-FTIR analysis of 3000-3800 cm^{-1} OH stretching vibration peak of glycerol in neat glycerol, glycerol in D_2O, and glycerol in CND; analysis of water state in (b) glycerol-CND and (c) glycerol-CND-D_2O mixtures, and the OH peak of (d) glycerol-CND, (e) glycerol-D_2O, and (f) glycerol-CND-D_2O

Another important effect is how the inorganic salt hydrate interacts with the hydroxyl group of PVA. Our group previously explored this question when PVA was dissolved in a different PCM – lithium nitrate trihydrate (LNH), using a deuterated analogue of LNH, LND.[17] In that paper, interaction of Li^+ and hydroxyl of PVA was confirmed by the frequency shift of the OH stretching vibrational peaks detected by FTIR

and the change of Li^+ mobility detected by Li^7 NMR before and after adding PVA into LND. In this study, blue shifts of the -OH peaks of glycerol were observed upon dilution of glycerol with either CND or D_2O, indicating a weakening of glycerol-glycerol hydrogen bonds due to increased interaction of glycerol molecules with solvent species (Fig. 3.4a). Interestingly, the addition of CND resulted in a more significant shift. We suggest that salt ions have played a more critical role in -OH peak shifting, and further we compared the observed trends with those seen in the glycerol-CND-D_2O system. Fig. 3.4d shows that in a two-component glycerol-CND system, a dramatic blue shift of the -OH vibrational band of glycerol occurs upon increase in CND content (a ~150 cm^{-1} shift between neat glycerol and 0.15 mole fraction of glycerol in CND at 0.17 mole fraction of $Ca(NO_3)_2$). These data suggest a strong interaction of partially hydrated Ca^{2+} with -OH group of glycerol. Whereas in glycerol-D_2O system, blue shift of the -OH vibrational band of glycerol occurs upon increase in D_2O content, 0.15 mole fraction of glycerol in D_2O shows a ~100 cm^{-1} blue shift when compared to neat glycerol (Fig. 3.4e). Under the same mole fraction of glycerol, stronger blue shift results due to CND when compared with D_2O, suggesting that the stronger shift related to the partial hydration of Ca^{2+}. The stronger disruption of glycerol-glycerol hydrogen bonding by CND as compared to water is also seen Fig. 3.4f. It is seen that the blue shift of the glycerol -OH stretching peak caused by a solvent is ~ ~50 cm^{-1} smaller in D_2O solutions as compared to that in CND solutions. Therefore, we believe there are strong interactions between Ca^{2+} and hydroxyl group of glycerol in glycerol-CND.

For PVA dissolved in CNH, a similar situation to glycerol will arise due to water scarcity in the system, leading to a competition between partially hydrated ions with polymers for water molecules. Therefore, a picture arises for Ca^{2+} cations interacting with hydroxyl groups of PVA, and the dehydrated PVA chains forming intermolecular hydrogen bonds, with both of these processes resulting in the formation of a physical gel (Fig. 3.5).

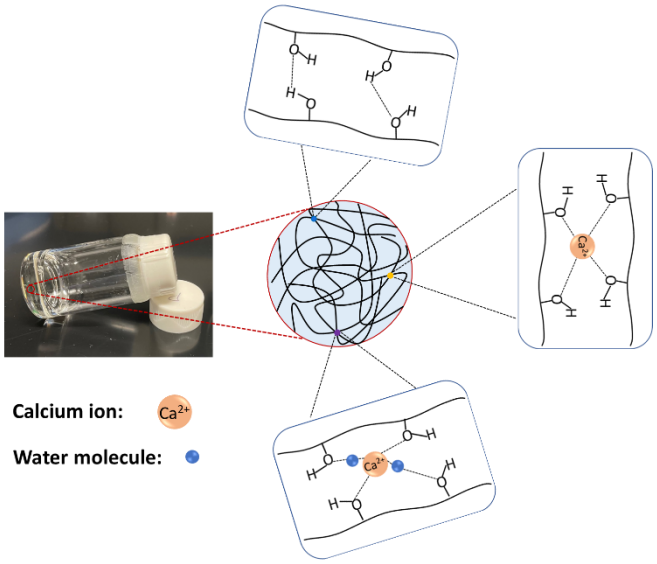

Figure 3.5. Schematic of suggested gelation mechanism of PVA in CNH

3.2. PVA gelation in CNH

A polymer gel is a 3D network structure of flexible chains crosslinking by chemical or physical bonds. The chain overlap is a necessary condition for gelation. Therefore, we are using 4 wt% of various PVA in CNH to demonstrate the rheological properties and the determination of T_{gel} (Fig. 3.6 and Fig. 3.7), to make sure all of them obtain the chain overlap situation in gel state.

Table 3.1 Abbreviation for different PVA used to make salogels

Abbreviation	Molecular weight	Hydrolysis degree
$PVA_{H,98}$	88 – 97 kg/mol	98%
$PVA_{M,98}$	57 – 66 kg/mol	98%
$PVA_{H,87}$	88 – 98 kg/mol	87%

Rheological experiments were performed to better understand the viscoelastic behavior of PVA in CNH. Strain sweep at a frequency of 10 rad/s was carried out to determine the linear viscoelastic regime. The gel-sol transition temperature (T_{gel}) was determined in oscillatory temperature sweep experiments from the crossover point of storage modulus (G') and loss modulus (G'') (Fig. 3.6). All the oscillatory temperature sweep measurements were conducted at a frequency of 10 rad/s and 6% strain. The viscoelastic behavior was studied in oscillatory shear experiments using the double logarithmic plots of dynamic storage moduli (G') and loss moduli (G'') as a function of angular frequency (ω). At low frequencies where G''(ω) > G'(ω), liquid-like behavior was dominant; as ω increased, G'(ω) gradually exceeded G''(ω), the elastic character became dominant, and gels showed a solid-like behavior. When G''(ω) = G'(ω), the system exhibited a sol-gel transition. Crossover modulus (G_c), crossover frequency (ω_c), and relaxation time ($\tau=1/\omega_c$) of the system are essential parameters to evaluate the crosslinking network of the gel. G_c and τ are related to the crosslinking degree and the crosslinking lifetime within the gel, respectively.[40]

In rheological experiments, we aimed to explore the effect of molecular weight and degree of hydrolysis of PVA on its gelation in CNH. To that end, a series of salogels

were prepared by adding a certain amount of PVA with different molecular weights and degrees of hydrolysis to CNH. Fig. 3.7 shows the effect of increasing molecular weights and degrees of hydrolysis on T_{gel} and strength of PVA/CNH salogels. Higher molecular weight results in larger connected junction zones, making it easier to form physical entanglements or connected polymer networks. Molecular weight effect on gelation has already been proven in many polymer systems,[41-43] and it also present in PVA/CNH system. Under the same PVA concentration, $PVA_{H,98}$ exhibited higher T_{gel} and larger τ than $PVA_{M,98}$ did, indicating that higher molecular weight of PVA forms stronger network structure.

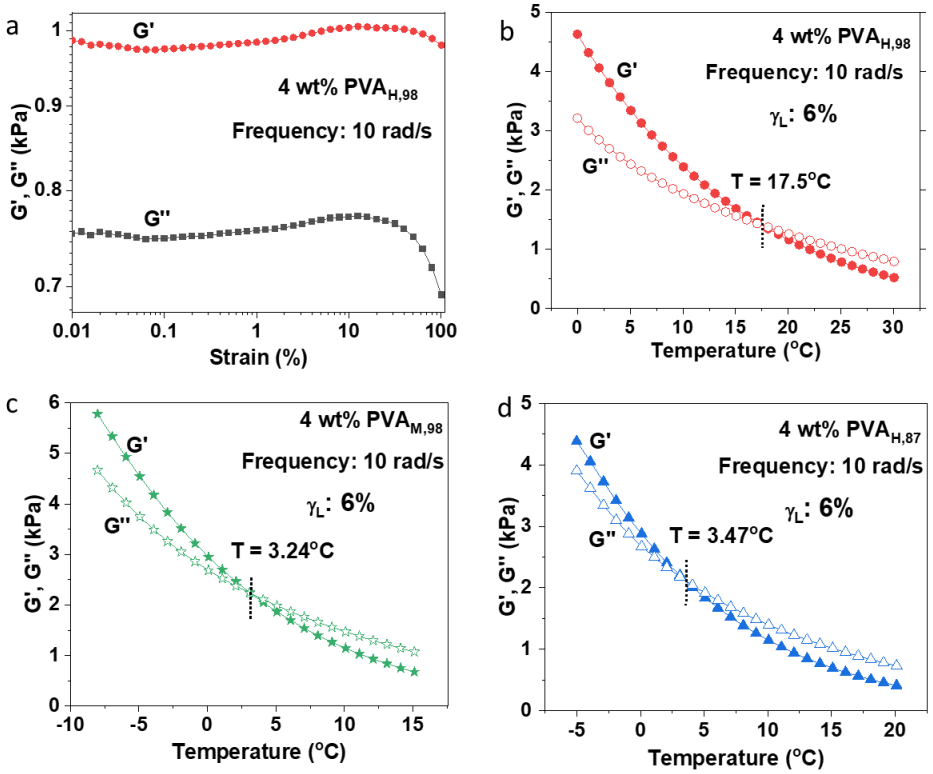

Figure 3.6. (a) Rheological experiments with 4 wt% PVA gels in CNH: Oscillation amplitude sweep in $PVAH_{,98}$ /CNH system at 25°C, and temperature sweep in (b) $PVA_{H,98}$/CNH (c) $PVA_{M,98}$/CNH and (d) $PVA_{H,98.}$ /CNH systems.

Interactions of PVA with other polar polymers or water are critical in forming physical crosslinking points to achieve the network structure. These interactions are expected to vary as a function of the degree of hydrolysis of PVA.[44, 45] The fact that higher T_{gel} and stronger gels are formed with PVA with higher degree of hydrolysis indicate the important role of intermolecular hydrogen bonding between PVA hydroxyl group during gelation. PVA with higher degree of hydrolysis provides more -OH group for forming physical crosslinking points, facilitating the formation of a 3D network. Inhibition of hydrogen bonding between PVA and water due to scarcity of water in the PVA/CNH system is enhancing such interactions. We suggest that both polymer-polymer hydrogen bonding and binding between cations and -OH of PVA are critical for gelation, according to the suggested gelation mechanism.

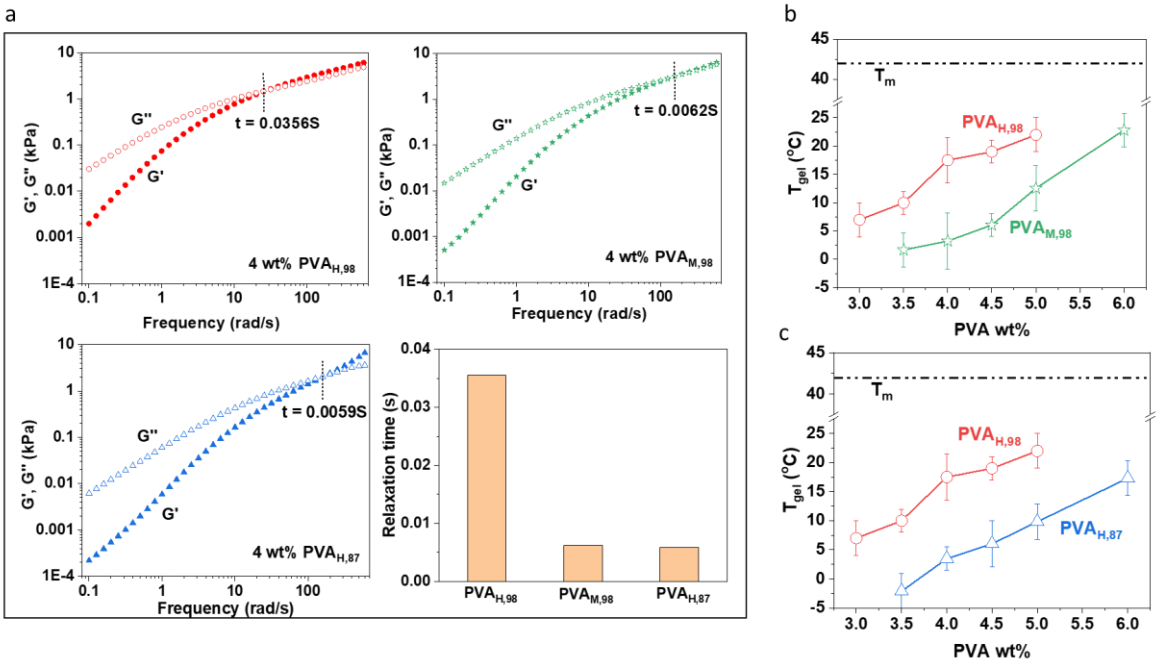

Figure 3.7. Effect of molecular weight and degree of hydrolysis of PVA on (a) strength of salogels and (b-c) T_{gel}.

Taken together, our results suggest that an increase in molecular weight and degree of hydrolysis of PVA results in stronger salogels with higher T_{gel}.. However, the salogels formed by dissolving PVA in CNH are relatively weak and exhibit low T_{gel}. For example, Salogels from by 5 wt% $PVA_{H,98}$ in CNH had T_{gel} of 22°C which was still far below the melting point of CNH (42°C).

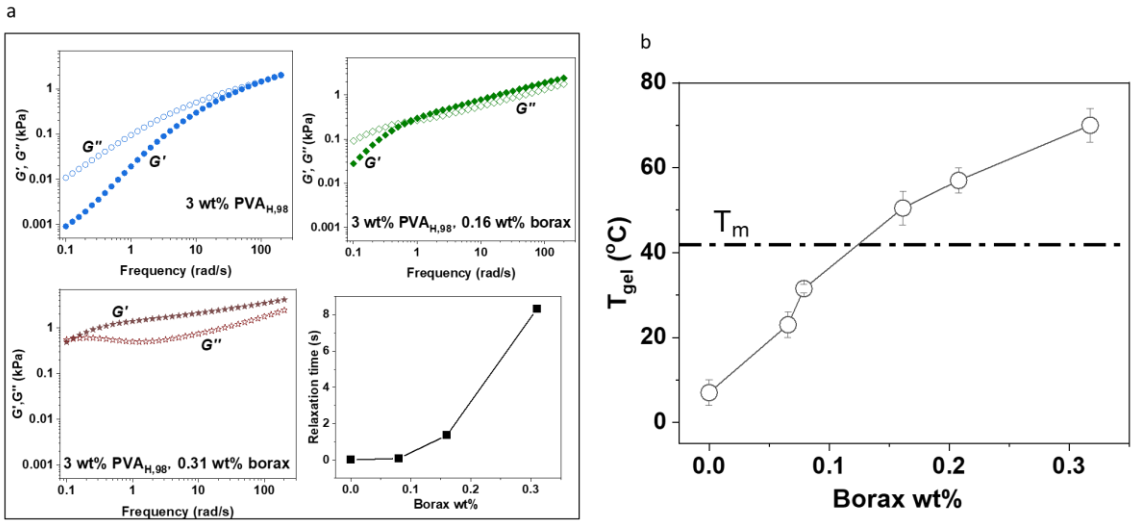

Figure 3.8. Effect of borax concentration on (a) rheological properties and (b) T_{gel} of a PVA/CNH salogel.

3.3. Borax as a crosslinker in PVA/CNH system

To achieve T_{gel} above melting point of CNH and strengthen the salogels, borax as a crosslinker was introduced. Because borax forms dynamic covalent bonds with the hydroxyl group of PVA, we expected that it would be able to maintain temperature-responsiveness of salogels. In the following experiments, the PVA we used is $PVA_{H,98}$. Fig. 3.8 shows that just a tiny amount of borax can improve T_{gel} dramatically and result in solgels with T_{gel} value higher than the melting point of CNH. Specifically, addition of 0.31 wt% borax to 3 wt% PVA/CNH system raised T_{gel} to 63°C and caused 3 orders of

magnitude increase in the relaxation time. Hence, borax is an effective crosslinker for PVA/CNH system that also supports temperature-responsive behavior to the salogel. The didiol-borax complex is in chemical equilibrium with boric acid, borate anion, and the PVA chain, and dissociates to the initial components with increasing temperature.[46]

Another feature brought in by the use of borax in PVA/CNH system is sensitivity to pH. Borax dissociates into boric acid and borate anion (equation 1-2), and there exist a dynamic equilibrium between these species. Neutral boric acid is favored in acid conditions, whereas in basic conditions, increase concentration of OH^- will shift the equilibrium towards formation of borate anion. The role of borate ions in forming borate ester bonds as crosslinking points and the formation of salogels was further explored by tuning the pH of PVA/borax/CNH system. We selected 3 wt% PVA/CNH salogel with 0.16% borax to compare its properties at its original pH (pH 6) and at higher pH. Ammonium hydroxide was used to tune the system pH instead of using strong base sodium hydroxide because sodium hydroxide led to precipitation of Ca^{2+}. The highest pH we could achieve with ammonium hydroxide in this system was pH 9. Frequency sweep experiments showed that G'(ω) exceeded G''(ω) in our test frequency range, 0.1-300 rad/s for salogels at pH>7, indicating that the crossover modulus occurred at a lower frequency resulting in τ longer than that for salogels at pH 6 (Fig. 3.9a). Therefore, raising pH can help the formation of additional borate ester bonds by converting boric acid to borate anions, resulting in salogel strengthening. In contrast, at increased pH, PVA/CNH salogels demonstrated a slight decrease of T_{gel} and gel weakening (Fig. 3.9b), probably because the addition of ammonium hydroxide solution introduced extra water in the system which

could weaken the gel due to dilution. As pH of PVA/borax/CNH salogel was raised from 6 to 7, T_{gel} increased by ~20 ^{o}C. However, further increase of pH to 8 or 9 did not show large effect on T_{gel} and strength of salogels. This is probably because most of boric acid had been already transformed to borate anion when pH was raised to 7. Therefore, shifting the equilibrium between boric acid and borate ions, and thus the density of dynamic crosslinking points by pH is a powerful means to controlling the network structure and tuning T_{gel} of the salogels.

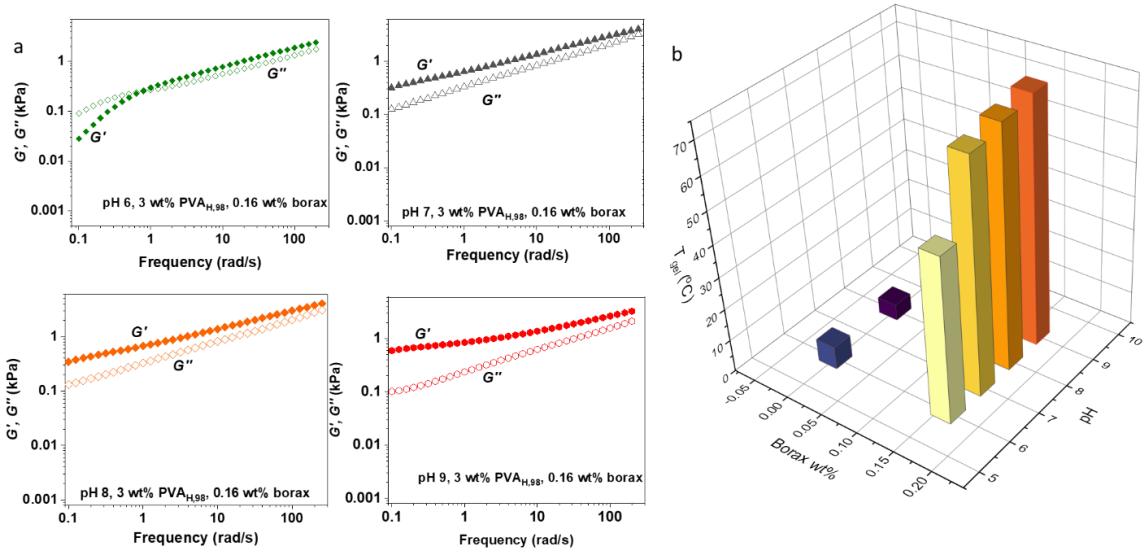

Figure 3.9. Effect of pH on (a) rheological properties and (b) T_{gel} of PVA/CNH and PVA/borax/CNH salogels.

It was interesting to compare PVA/borax/CNH salogels with similar aqueous systems. The capability of borax to form dynamic covalent borate ester bonds with -OH groups of PVA has been widely used as an efficient way of strengthening PVA-based hydrogels.[30, 40, 47, 48] Some investigations show that in PVA-borax aqueous systems, the addition of salt ions can result in an intrinsic viscosity decrease and/or phase separation instead of gelation. The chain expansion of PVA-borax complex has been shown to be

limited by the ions shielding effect due to its polyelectrolyte behavior.[49-51] However, borax-assisted gelation of PVA in a molten salt hydrate solvent is reported here to the best of our knowledge for the first time.

3.4. Comparison of PVA-borax in CNH versus H_2O

In PVA/borax/H_2O hydrogel system, the pH-responsiveness has been extensively studied.[27, 52] It was demonstrated that in basic conditions, equilibrium between boric acid and borate ions is shifted towards the formation of the borate ions, inducing stronger networks. Conversely, acidic conditions favor formation of boric acid, and result in weaker networks. In our work, PVA/borax/CNH salogels could be strengthened by an increase in pH, and the salogels could be destroyed by adding hydrochloric acid (Fig. 3.10).

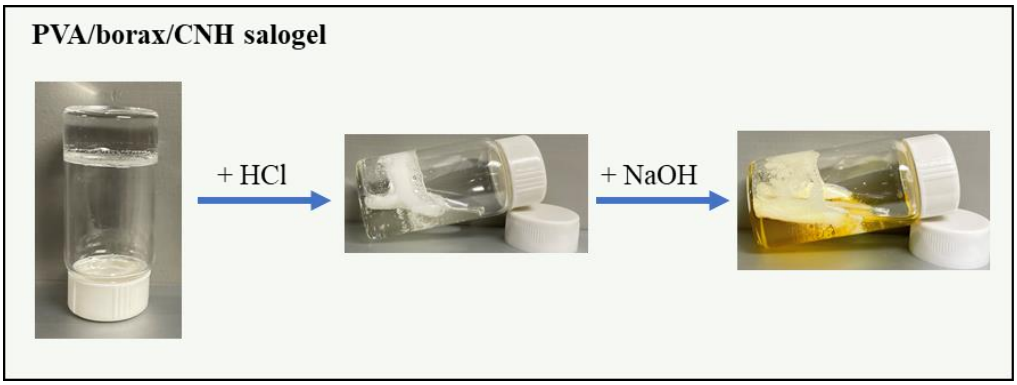

Figure 3.10. PVA/borax/CNH salogel behavior in tuning pH experiment

Figure 3.11. PVA/ CNH salogel behavior in tuning pH experiment

However, unlike temperature response of PVA/borax/CNH salogels, pH response was not repeatable. After the PVA/borax/CNH salogels have been destroyed by acid, they could not recover by adding base. A similar phenomenon was observed in PVA/CNH salogels (Fig 3.11). Destruction of the PVA networks in PVA/borax/CNH salogels with an acid can be used for PCM removal from heat storage modules.

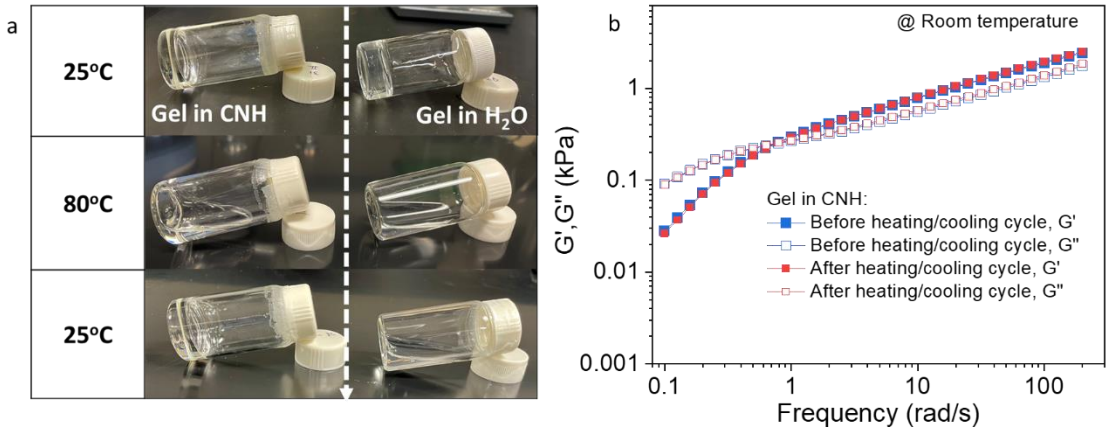

Figure 3.12. Comparison of thermo-reversibility of PVA/borax/CNH salogel and PVA/borax/H_2O systems shown before and after heating at 80°C for 24 hours. (a) visualized and (b) rheologically in a demonstration experiment.

In this work, however, we were more interested in temperature stimulation of salogels. Note that for PVA/borax/H_2O hydrogels, repeatability of temperature stimulation is not as well explored as pH-responsiveness. Therefore, we aimed to compare thermal properties in PVA/borax/H_2O hydrogel and PVA/borax/CNH salogel systems. Fig. 3.12a shows that 24-hour exposure of PVA/borax/CNH salogels and PVA/borax/H_2O hydrogels to 80°C transformed both systems into liquids. However, PVA/borax/CNH salogels could nearly totally recover upon cooling to room temperature, while PVA/borax/H_2O gels remained liquid under the same conditions. Fig. 3.12b shows that rheological properties

of PVA/borax/CNH salogels remained almost the same before and after the heating/cooling cycle.

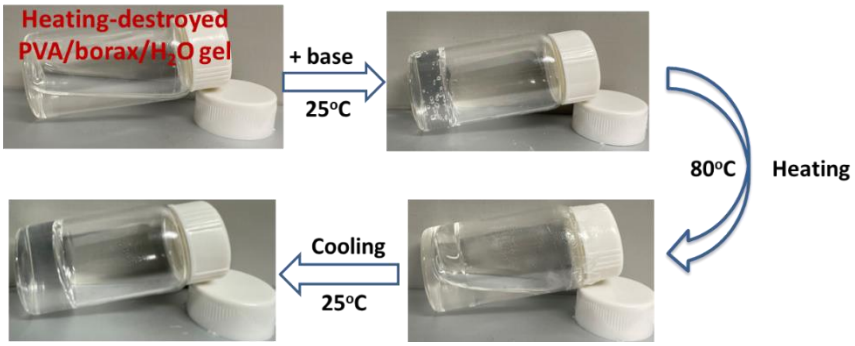

Figure 3.13. Destroyed PVA/borax/H_2O system behavior after adding base.

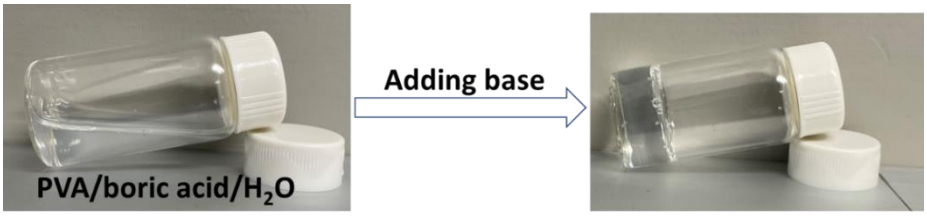

Figure 3.14. PVA/boric acid/H_2O behavior before and after adding base at room temperature.

However, addition of a base (such as sodium hydroxide) to a heating-destroyed PVA/borax/H_2O gel, led to gelation and recovery of temperature reversibility (Fig. 3.13). Consequently, we suggest that recovery of PVA/borax/H_2O gels after heating is dependent on the equilibrium between borate ions and boric acid, whose kinetics is affected by temperature and ionic strength,[53, 54] and whose thermodynamics is strongly dependent on pH. Interestingly, a control experiment which involved addition of boric acid to PVA aqueous solutions revealed that no gelation was observed before the addition of sodium hydroxide to this system (Fig. 3.14), indicating that the effect of boric acid on gelation is negligible. Therefore, we suggest that in PVA/borax/H_2O hydrogels at neutral

pH, borate ions are transformed to boric acid during heating, and the gelation therefore does not occur upon cooling. However, in PVA/borax/CNH salogels at pH 6, high concentrations of ions and scarcity of water dramatically affect the equilibrium between boric acid and borate ion favoring formation of borate ions, enabling temperature repeatability. To the best of our knowledge, these reported results are the first example of PVA-borax-based gels showing temperature-repeatability at a neutral pH.

3.5. Shape stabilization and heat of fusion of PVA/borax/CNH salogels

The ultimate application of the salogels studies in this work is shape stabilization of CNH during its freezing/melting cycles. To easily fill in or remove CNH from the thermal storage units, salogels must be able to flow at high temperatures, but remain in their gel state and prevent leakage of CNH at temperature that are moderately higher than the CNH melting temperature. To demonstrate the capability of PVA/borax salogels to provide shape stabilization for molten CNH we performed an experiment which is illustrated in Fig. 3.15. First, a salogel of 3 wt % PVA and 0.31 wt% borax in CNH was prepared below the melting point of CNH. Such a salogel appears white due to crystallization of CNH. When PVA/borax/CNH salogel was then heated to 50^{o}C, it turned transparent as a result of melting of CNH crystals. Importantly, the PVA network effectively entrapped molten CNH, ultimately inhibiting leakage of CNH above its T_m of 42^{o}C and maintained the shape for at least 2 hours. In comparison, neat molten CNH was highly fluid due to its low viscosity.[55] When the salogel was further heated above its T_{gel} of 70^{o}C, the salogel transformed to liquid and started to flow. These experiments show that robust PVA/borax/CNH salogels with low polymer concentration and crosslinker

content, can entrap and prevent leakage of large amounts of CNH during melting/freezing cycles of this PCM.

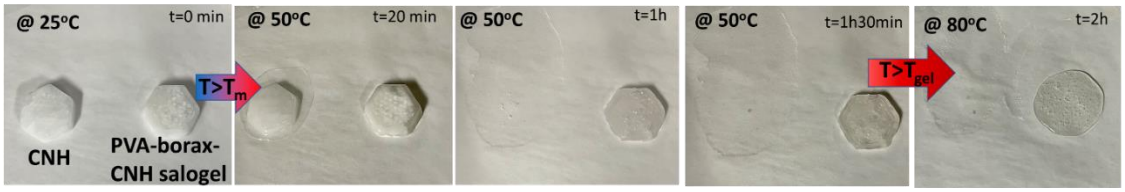

Figure 3.15. Melting of neat CNH and shape stabilization of neat CNH in PVA/borax/CNH salogels at 50°C. Gel-sol transition of PVA-borax-CNH salogel at 80°C.

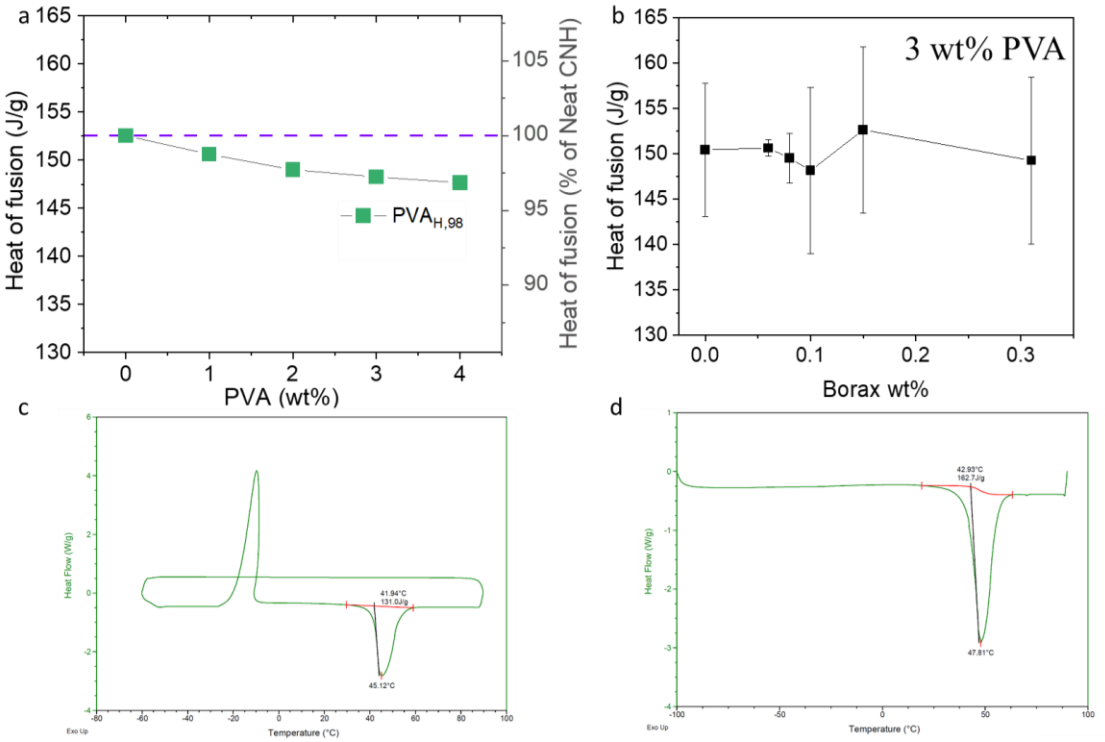

Figure 3.16. Heat of fusion measured by DSC for (a) PVA/CNH and (b) PVA/borax/CNH salogels; DSC curves for (c) neat CNH and (d) 3 wt% PVA, 0.31 wt% borax salogel.

For the use of CNH-based salogels in heat storage applications, preservation of a high heat of fusion of salogels compared to that of neat CNH is critically important. Because the DSC curves were run at different times (Fig. 3.16 c & d), the calorimeter

chips have been calibrated during this time, so we normalized all the dates into primary standards for comparison. The heat of fusion obtained from analysis of DSC data of PVA/CNH salogels is shown in Fig. 3.16a. A reduction of heat of fusion of neat CNH was approximately proportional to the amount of added PVA. The observed changes indicate that the heat of fusion decreased mainly due to dilution of CNH by PVA, and the interaction between PVA and CNH did not play a significant role in the heat of fusion of the PVA/borax/CNH salogel system.

Fig. 3.16b shows the effect of borax on heat of fusion of salogels, the addition of borax will cause fluctuation of the heat of fusion of salogels. This may be because borax will introduce other ions like sodium ion and borate ion into the system, which could affect the composition of crystal CNH, thus causing a little fluctuation of the heat of fusion. However, the borax amount added is very small, therefore robust PVA/borax/CNH salogel can maintain high percentage heat of fusion compared to neat CNH. Overall, the PVA/borax/CNH salogel not only solve the leakage problem of CNH but also have high heat of fusion.

3.6. Self-healing properties of PVA/borax/CNH salogels.

Physical gels and PVA/borax/H_2O hydrogels show self-healing properties which are supported by the transient nature of reversible crosslinking points.[56-58] To explore the self-healing properties of PVA/borax/CNH salogels, step strain experiments probing recovery of mechanical properties of the salogels after a network rupture were performed.

First, a simple strain amplitude test was conducted on PVA/borax/CNH salogels to find the linear and non-linear regions of strain magnitude limits for network recovery

and breaking, respectively. Then, step strain measurements were performed between 300% and 10% strain to explore the rupture and recovery of the loss modulus and storage modulus of the salogels. In Fig. 3.17a-b, the salogels quickly recovered under 10% strain after rupturing under 300% strain. In Fig 3.18c, two pieces of PVA/borax/CNH salogels completely healed after been brought in contact for 10 min at room temperature. The healed salogels could be stretched up to >300% without breaking, confirming the self-healing property. The self-healing ability of the PVA/borax/CNH salogels is supported by the dynamic nature of hydrogen bonds and covalent borate ester bonds in this system.

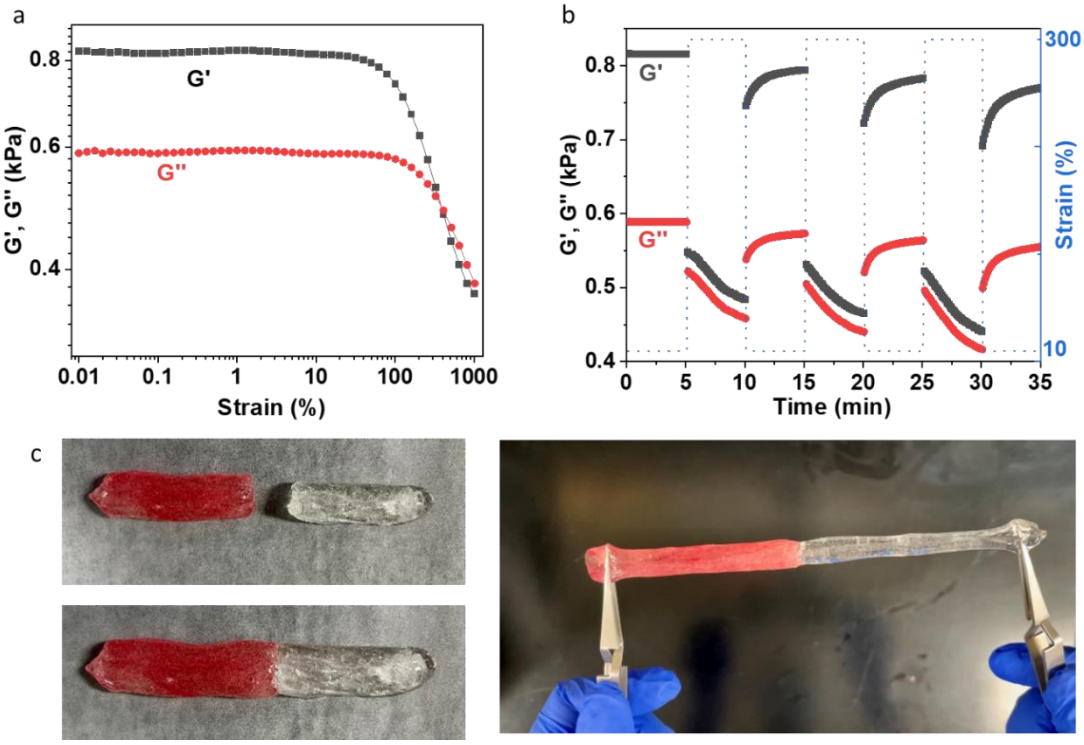

Figure 3.17. Self-healing of salogels (a-b) demonstrated rheologically and (c) visualized in a demonstration experiment.

4. CONCLUSIONS

In this study, temperature responsive, tunable T_{gel}, and self-healing salogels were introduced for trapping an inorganic phase change material (CNH) during its melting/freezing cycles to overcome its leakage problem. The gelation mechanism of PVA in CNH was studied by using ATR-FTIR in the model systems which contained glycerol instead of PVA. D_2O was used to make CND to separate the -OH peak of glycerol from -OD peak of D_2O. Analysis of -OD stretching vibrations of D_2O and -OH stretching vibrations of glycerol at varied CND content in glycerol-CND and glycerol-CND-D_2O systems revealed the dehydrated state of -OH groups of glycerol and PVA in CNH, and the central role of such dehydration in gel formation.

It was shown that PVA with higher molecular weights and higher degrees of hydrolysis provided stronger salogel network structures but still weak gel. The use of borax as a physical crosslinker forming dynamic covalent bonds with PVA strengthens the salogels and improved their T_{gel}. Through variations of PVA and borax concentrations, as well as pH, T_{gel} of PVA/borax/CNH salogels could be tuned in range of 7^{o}C-70^{o}C. The use of PVA in combination with borax provides an effective means for shape stabilization of CNH during it cooling/melting transitions. Low concentration of the polymer and the crosslinker required for the formation of a strong hydrogel network structure, which enabled the retention of high heat of fusion by the PVA/borax/CNH salogel system compared to the neat CNH. Furthermore, PVA/borax/CNH salogels showed unique, repeatable thermo-reversible properties not achievable with PVA/borax/H_2O hydrogel

systems. We believe that these unique properties are related to the unique environment provided by CNH. Moreover, PVA/borax/CNH salogels exhibited self-healing capability which is supported by the dynamic nature of the reversible crosslinking points.

Future work will focus on applying PVA-borax salogels to other inorganic salt hydration PCMs and eutectics, while also elucidating the gelation mechanism.

5. REFERENCES

1. Alva, G.; Lin, Y.; Fang, G., An overview of thermal energy storage systems. *Energy* **2018,** *144*, 341-378.

2. Su, W.; Darkwa, J.; Kokogiannakis, G., Review of solid–liquid phase change materials and their encapsulation technologies. *Renewable and Sustainable Energy Reviews* **2015,** *48*, 373-391.

3. Sharma, A.; Tyagi, V. V.; Chen, C.; Buddhi, D., Review on thermal energy storage with phase change materials and applications. *Renewable and Sustainable energy reviews* **2009,** *13* (2), 318-345.

4. Zalba, B.; Marın, J. M.; Cabeza, L. F.; Mehling, H., Review on thermal energy storage with phase change: materials, heat transfer analysis and applications. *Applied thermal engineering* **2003,** *23* (3), 251-283.

5. Moynihan, C. T., A low temperature fused salt experiment: The conductivity, viscosity, and density of molten calcium nitrate tetrahydrate. *Journal of Chemical Education* **1967,** *44* (9), 531.

6. Karimineghlani, P.; Emmons, E.; Green, M. J.; Shamberger, P.; Sukhishvili, S. A., A temperature-responsive poly (vinyl alcohol) gel for controlling fluidity of an inorganic phase change material. *Journal of Materials Chemistry A* **2017,** *5* (24), 12474-12482.

7. Karimineghlani, P.; Palanisamy, A.; Sukhishvili, S. A., Self-Healing Phase Change Salogels with Tunable Gelation Temperature. *ACS applied materials & interfaces* **2018,** *10* (17), 14786-14795.

8. Alipoori, S.; Mazinani, S.; Aboutalebi, S. H.; Sharif, F., Review of PVA-based gel polymer electrolytes in flexible solid-state supercapacitors: Opportunities and challenges. *journal of energy storage* **2020,** *27*, 101072.

9. Otsuka, E.; Suzuki, A., A simple method to obtain a swollen PVA gel crosslinked by hydrogen bonds. *Journal of applied polymer science* **2009,** *114* (1), 10-16.

10. Matsumura, S.; Tomizawa, N.; Toki, A.; Nishikawa, K.; Toshima, K., Novel poly (vinyl alcohol)-degrading enzyme and the degradation mechanism. *Macromolecules* **1999,** *32* (23), 7753-7761.

11. Silva, G.; Sobral, P.; Carvalho, R.; Bergo, P.; Mendieta-Taboada, O.; Habitante, A., Biodegradable films based on blends of gelatin and poly (vinyl alcohol): effect of PVA type or concentration on some physical properties of films. *Journal of Polymers and the Environment* **2008,** *16* (4), 276-285.

12. Bercea, M.; Morariu, S.; Rusu, D., In situ gelation of aqueous solutions of entangled poly (vinyl alcohol). *Soft Matter* **2013,** *9* (4), 1244-1253.

13. Maitra, J.; Shukla, V. K., Cross-linking in hydrogels-a review. *Am. J. Polym. Sci* **2014,** *4* (2), 25-31.

14. Alves, M. H.; Jensen, B. E.; Smith, A. A.; Zelikin, A. N., Poly (vinyl alcohol) physical hydrogels: new vista on a long serving biomaterial. *Macromolecular bioscience* **2011,** *11* (10), 1293-1313.

15. Narita, T.; Indei, T., Microrheological study of physical gelation in living polymeric networks. *Macromolecules* **2016,** *49* (12), 4634-4646.

16. Zhang, Y.; Huang, W.; Zhou, Y.; Yan, D., A physical gel made from hyperbranched polymer gelator. *Chemical communications* **2007,** (25), 2587-2589.

17. Karimineghlani, P.; Zheng, J.; Hu, Y.-Y.; Sukhishvili, S., Solvation and diffusion of poly (vinyl alcohol) chains in a hydrated inorganic ionic liquid. *Physical Chemistry Chemical Physics* **2020,** *22* (31), 17705-17712.

18. Xu, M.; Larentzos, J. P.; Roshdy, M.; Criscenti, L. J.; Allen, H. C., Aqueous divalent metal–nitrate interactions: hydration versus ion pairing. *Physical Chemistry Chemical Physics* **2008,** *10* (32), 4793-4801.

19. Smirnov, P.; Yamagami, M.; Wakita, H.; Yamaguchi, T., An X-ray diffraction study on concentrated aqueous calcium nitrate solutions at subzero temperatures. *Journal of molecular liquids* **1997,** *73*, 305-316.

20. Ribeiro, M. C., Polarization effects in molecular dynamics simulations of glass-formers Ca (NO 3) 2· n H 2 O, n= 4, 6, and 8. *The Journal of chemical physics* **2010,** *132* (13), 134512.

21. Igarashi, K.; Tajiri, K.; Asahina, T.; Kosaka, M.; Iwadate, Y.; Mochinaga, J., X-ray diffraction study of calcium nitrate tetrahydrate melt at 328 K. *Journal of materials science* **1993,** *28* (10), 2774-2778.

22. Zhang, Y.; Li, Y.; Liu, W., Dipole‐dipole and H‐bonding interactions significantly enhance the multifaceted mechanical properties of thermoresponsive shape memory hydrogels. *Advanced Functional Materials* **2015,** *25* (3), 471-480.

23. Liang, R.; Yu, H.; Wang, L.; Lin, L.; Wang, N.; Naveed, K.-u.-R., Highly tough hydrogels with the body temperature-responsive shape memory effect. *ACS applied materials & interfaces* **2019,** *11* (46), 43563-43572.

24. Li, Z.; Shen, J.; Ma, H.; Lu, X.; Shi, M.; Li, N.; Ye, M., Preparation and characterization of pH-and temperature-responsive nanocomposite double network hydrogels. *Materials Science and Engineering: C* **2013,** *33* (4), 1951-1957.

25. Liu, C.; Lei, F.; Li, P.; Wang, K.; Jiang, J., A review on preparations, properties, and applications of cis-ortho-hydroxyl polysaccharides hydrogels crosslinked with borax. *International Journal of Biological Macromolecules* **2021**.

26. He, L.; Szopinski, D.; Wu, Y.; Luinstra, G. A.; Theato, P., Toward self-healing hydrogels using one-pot thiol–ene click and borax-diol chemistry. *ACS Macro Letters* **2015,** *4* (7), 673-678.

27. Lu, B.; Lin, F.; Jiang, X.; Cheng, J.; Lu, Q.; Song, J.; Chen, C.; Huang, B., One-pot assembly of microfibrillated cellulose reinforced PVA–borax hydrogels with self-healing and pH-responsive properties. *ACS Sustainable Chemistry & Engineering* **2017,** *5* (1), 948-956.

28. Rezvan, G.; Pircheraghi, G.; Bagheri, R., Curcumin incorporated PVA‐borax dual delivery hydrogels as potential wound dressing materials—Correlation between

viscoelastic properties and curcumin release rate. *Journal of Applied Polymer Science* **2018,** *135* (45), 46734.

29. Seidi, F.; Jin, Y.; Han, J.; Saeb, M. R.; Akbari, A.; Hosseini, S. H.; Shabanian, M.; Xiao, H., Self‐healing Polyol/Borax Hydrogels: Fabrications, Properties and Applications. *The Chemical Record* **2020,** *20* (10), 1142-1162.

30. Lin, H.-L.; Liu, Y.-F.; Yu, T. L.; Liu, W.-H.; Rwei, S.-P., Light scattering and viscoelasticity study of poly (vinyl alcohol)–borax aqueous solutions and gels. *Polymer* **2005,** *46* (15), 5541-5549.

31. Pezron, E.; Leibler, L.; Ricard, A.; Audebert, R., Reversible gel formation induced by ion complexation. 2. Phase diagrams. *Macromolecules* **1988,** *21* (4), 1126-1131.

32. Dixit, A.; Bag, D. S.; Sharma, D. K.; Eswara Prasad, N., Synthesis of multifunctional high strength, highly swellable, stretchable and self‐healable pH‐responsive ionic double network hydrogels. *Polymer International* **2019,** *68* (3), 503-515.

33. Gao, L.; Guo, G.; Liu, M.; Tang, Z.; Xie, L.; Huo, Y., Multi-responsive, bidirectional, and large deformation bending actuators based on borax cross-linked polyvinyl alcohol derivative hydrogel. *RSC advances* **2017,** *7* (63), 40005-40014.

34. Sun, Q., The Raman OH stretching bands of liquid water. *Vibrational Spectroscopy* **2009,** *51* (2), 213-217.

35. Choe, C.; Lademann, J.; Darvin, M. E., Depth profiles of hydrogen bound water molecule types and their relation to lipid and protein interaction in the human stratum corneum in vivo. *Analyst* **2016,** *141* (22), 6329-6337.

36. Sun, Q.; Guo, Y., Vibrational sum frequency generation spectroscopy of the air/water interface. *Journal of Molecular Liquids* **2016,** *213*, 28-32.

37. Ludwig, R., Water: From clusters to the bulk. *Angewandte Chemie International Edition* **2001,** *40* (10), 1808-1827.

38. Tsai, C.; Jordan, K., Theoretical study of small water clusters: low-energy fused cubic structures for (H2O) n, n= 8, 12, 16, and 20. *The Journal of Physical Chemistry* **1993,** *97* (20), 5208-5210.

39. Zhao, T.; Xing, J.; Dong, Z.; Tang, Y.; Pu, W., Synthesis of polyacrylamide with superb salt-thickening performance. *Industrial & Engineering Chemistry Research* **2015,** *54* (43), 10568-10574.

40. Han, J.; Lei, T.; Wu, Q., High-water-content mouldable polyvinyl alcohol-borax hydrogels reinforced by well-dispersed cellulose nanoparticles: Dynamic rheological properties and hydrogel formation mechanism. *Carbohydrate polymers* **2014,** *102*, 306-316.

41. Shen, D.; Wan, C.; Gao, S., Molecular weight effects on gelation and rheological properties of konjac glucomannan–xanthan mixtures. *Journal of Polymer Science Part B: Polymer Physics* **2010,** *48* (3), 313-321.

42. Zhang, H.; Yoshimura, M.; Nishinari, K.; Williams, M.; Foster, T.; Norton, I., Gelation behaviour of konjac glucomannan with different molecular weights. *Biopolymers: Original Research on Biomolecules* **2001,** *59* (1), 38-50.

43. Tan, H.; Moet, A.; Hiltner, A.; Baer, E., Thermoreversible gelation of atactic polystyrene solutions. *Macromolecules* **1983,** *16* (1), 28-34.

44. Muppalaneni, S.; Omidian, H., Polyvinyl alcohol in medicine and pharmacy: a perspective. *J. Dev. Drugs* **2013,** *2* (3), 1-5.

45. Solaro, R.; Corti, A.; Chiellini, E., Biodegradation of poly (vinyl alcohol) with different molecular weights and degree of hydrolysis. *Polymers for Advanced Technologies* **2000,** *11* (8‐12), 873-878.

46. Koga, K.; Takada, A.; Nemoto, N., Dynamic light scattering and dynamic viscoelasticity of poly (vinyl alcohol) in aqueous borax solutions. 5. Temperature effects. *Macromolecules* **1999,** *32* (26), 8872-8879.

47. Huang, M.; Hou, Y.; Li, Y.; Wang, D.; Zhang, L., High performances of dual network PVA hydrogel modified by PVP using borax as the structure-forming accelerator. *Designed monomers and polymers* **2017,** *20* (1), 505-513.

48. Dixit, A.; Bag, D. S.; Kalra, S., Synthesis of strong and stretchable double network (DN) hydrogels of PVA-borax and P (AM-co-HEMA) and study of their swelling kinetics and mechanical properties. *Polymer* **2017,** *119*, 263-273.

49. Ochiai, H.; Kurita, Y.; Murakami, I., Viscosity behavior of the polyelectrolyte poly (vinyl alcohol) having some intrachain crosslinks. *Die Makromolekulare Chemie: Macromolecular Chemistry and Physics* **1984,** *185* (1), 167-172.

50. Keita, G.; Ricard, A.; Audebert, R.; Pezron, E.; Leibler, L., The poly (vinyl alcohol)-borate system: influence of polyelectrolyte effects on phase diagrams. *Polymer* **1995,** *36* (1), 49-54.

51. Lin, H.-L.; Liu, W.-H.; Liu, Y.-F.; Cheng, C.-H., Complexation equilibrium constants of poly (vinyl alcohol)-borax dilute aqueous solutions–consideration of electrostatic charge repulsion and free ions charge shielding effect. *Journal of Polymer Research* **2002,** *9* (4), 233-238.

52. Chung, W. Y.; Lee, S. M.; Koo, S. M.; Suh, D. H., Surfactant‐free thermochromic hydrogel system: PVA/borax gel networks containing pH‐sensitive dyes. *Journal of applied polymer science* **2004,** *91* (2), 890-893.

53. Zeebe, R. E.; Sanyal, A.; Ortiz, J. D.; Wolf-Gladrow, D. A., A theoretical study of the kinetics of the boric acid–borate equilibrium in seawater. *Marine Chemistry* **2001,** *73* (2), 113-124.

54. Waton, G.; Mallo, P.; Candau, S., Temperature-jump rate study of the chemical relaxation of aqueous boric acid solutions. *The Journal of Physical Chemistry* **1984,** *88* (15), 3301-3305.

55. Moynihan, C. T., The temperature dependence of transport properties of ionic liquids. The conductance and viscosity of calcium nitrate tetrahydrate and sodium thiosulfate pentahydrate. *The Journal of Physical Chemistry* **1966,** *70* (11), 3399-3403.

56. Yang, Y.; Urban, M. W., Self-healing polymeric materials. *Chemical Society Reviews* **2013,** *42* (17), 7446-7467.

57. de Greef, T. F.; Meijer, E., Supramolecular polymers. *Nature* **2008,** *453* (7192), 171-173.

58. Zhao, Z.; Liu, Y.; Zhang, K.; Zhuo, S.; Fang, R.; Zhang, J.; Jiang, L.; Liu, M., Biphasic synergistic gel materials with switchable mechanics and self‐healing capacity. *Angewandte Chemie* **2017,** *129* (43), 13649-13654.